Supplementary Fig. 1: PCR analysis of transgene integration into genomic DNA.

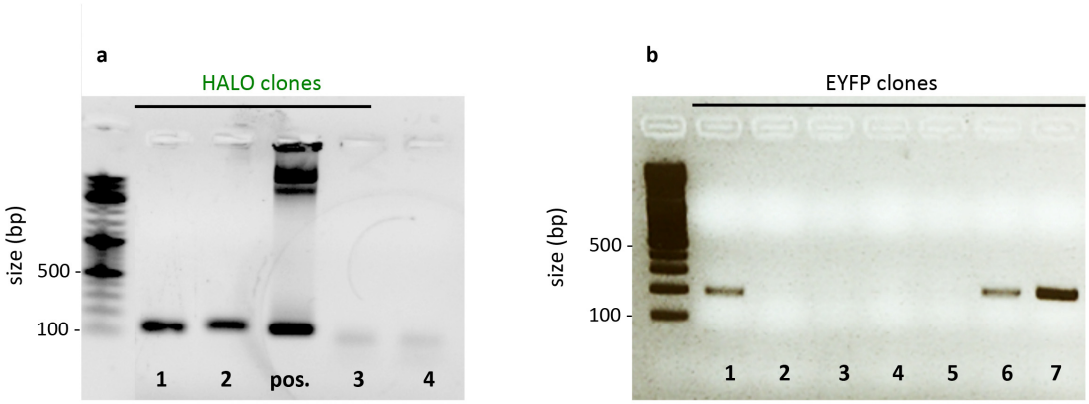

After transduction with *hSyn-eNpHR3.0-EYFP* or *hSyn-EYFP* lentivirus, emerging clones were harvested to screen genomic DNA for integration of transgenes. (**a**) *eNpHR3.0-EYFP* (HALO) harboring clones show a PCR product of 190 bp. (**b**) EYFP harboring clones show a PCR product of 187 bp. Molecular size marker in base pairs (bp).

Supplementary Fig. 2: Immunocytochemistry of differentiating HALO / EYFP lines.

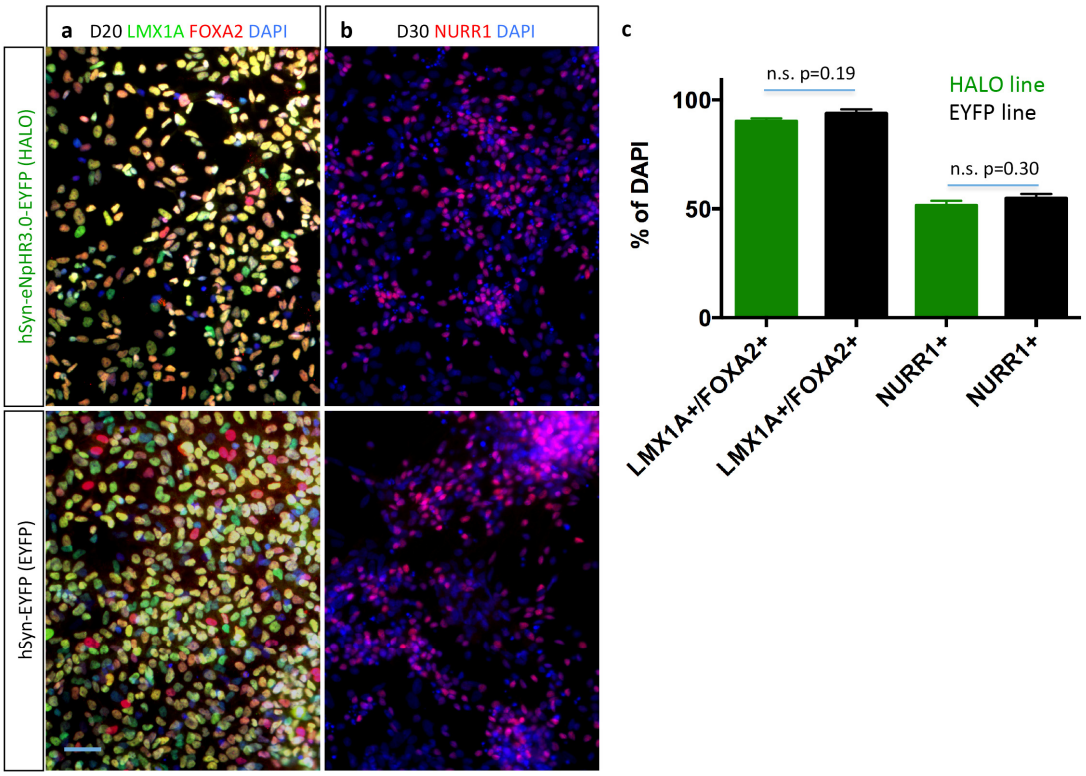

(**a**) At day (D) 20, more than 90% of cells in both lines express LMX1A (green) and FOXA2 (red). (**b**) At D30, about 50% of cells express the definitive dopamine marker NR4A2 (NURR1, red) in both lines. (**c**) Quantification of fates in (**a**) and (**b**), EYFP cells vs. HALO cells are not statistically different (t-test for LMX1A/FOXA2 expression t = 1.56, p = 0.19, n.s.; t-test for NURR1 expression t = 1.18, p = 0.30, n.s.). Scale bar 50 µm.

Supplementary Fig. 3: Immunocytochemistry of differentiating HALO / EYFP lines.

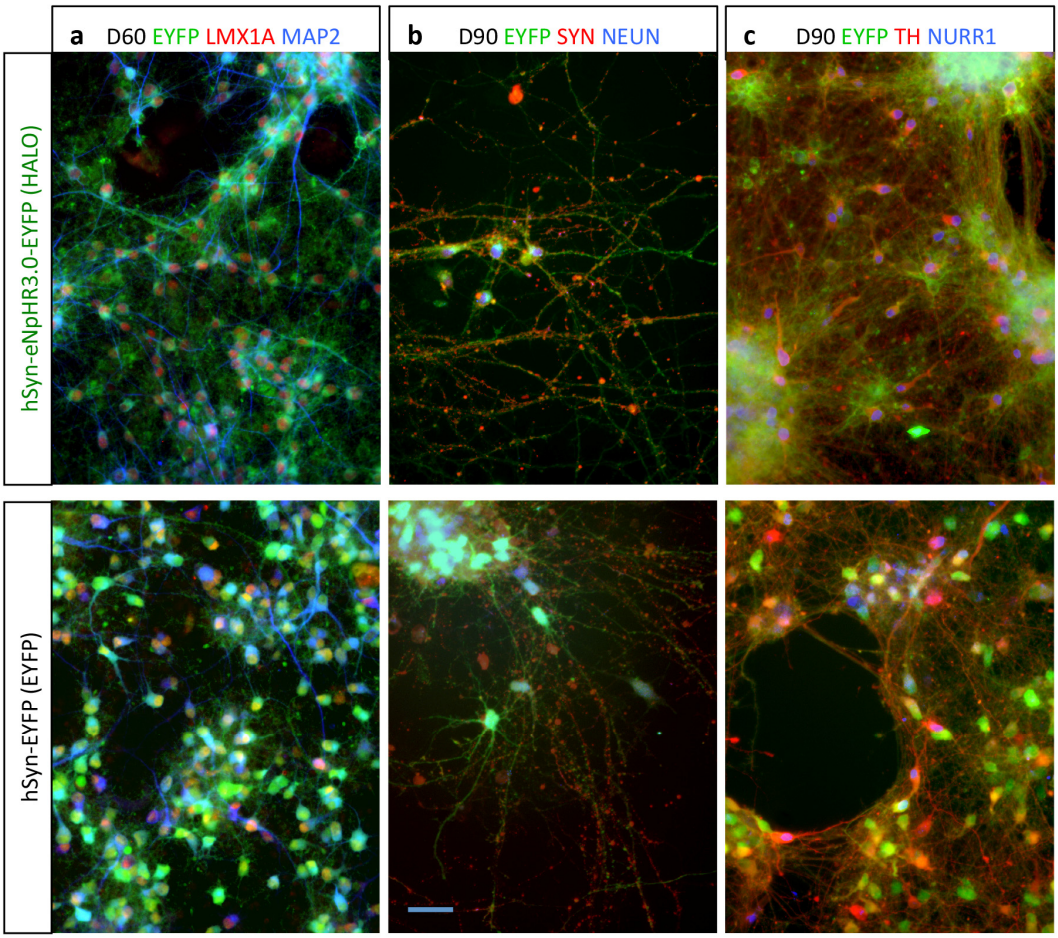

(**a**) At day (D) 60, neurons from both lines express LMX1A (red) and MAP2 (blue) and extend a dense EYFP+ fiber network (green). (**b**) By day 90, neurons express NEUN (blue) and Synaptophysin+ punctae (red) can be detected alongside EYFP+ fibers. (**c**) At day 90, cellular composition of TH+/NURR1+ expressing neurons and transgene expression is maintained in both lines. Scale bar 50 µm.

Supplementary Fig. 4: *In vitro* physiologic assessment of optogenetic control.

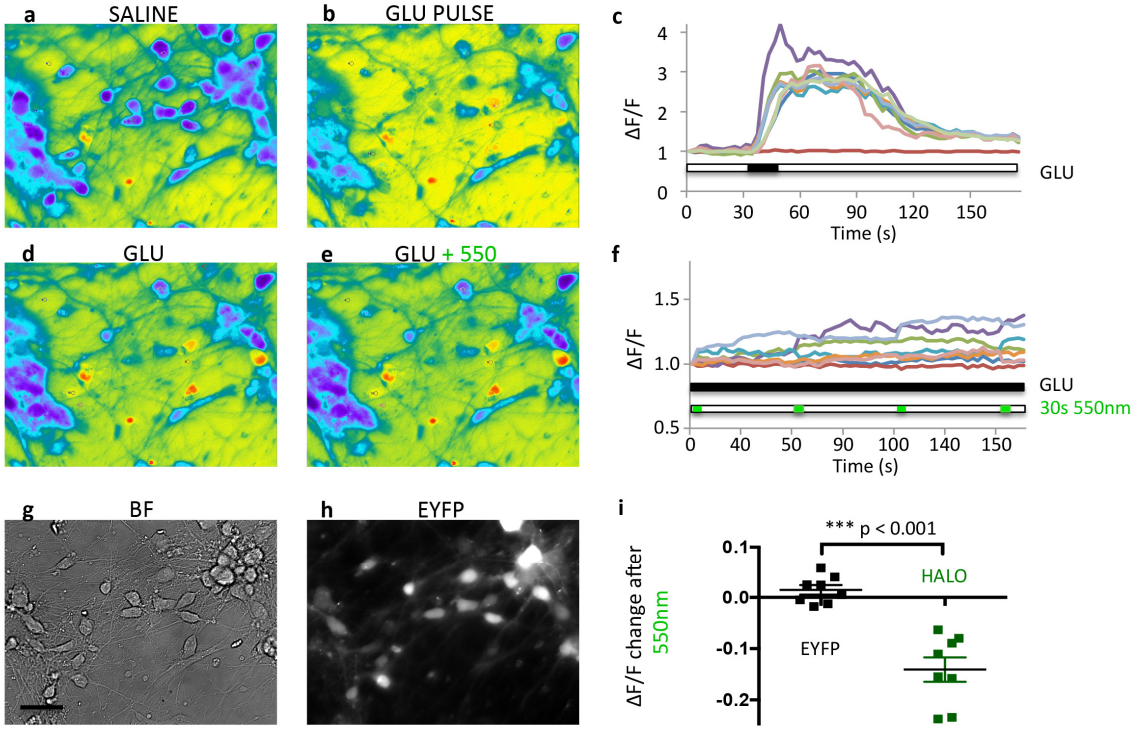

(**a**) Ratiometric image of a day 90 EYFP expressing mesDA-rich culture after incubation with 5 µm Fura-2. (**b**) A glutamate pulse (GLU, 100 µM) generated a calcium response in neurons as quantified in (**c**). During continuous glutamate perfusion (GLU, 50 µM, **d**) 550 nm light pulses (**e**) did not generate a significant change in calcium signal, quantified in (**f**)**.** (**g**) Shows bright field and (**h**) EYFP capture of this region. Scale bars 20 µm. (**i**) Quantification of the calcium reaction in response to 30 s 550 nm light pulses in EYFP vs. HALO cultures (EYFP +1.4 ± 0.9 %; HALO -14.0 ± 2.3 %, t-test $t = 6.07$, $p < 0.001$).

Supplementary Fig. 5: Immunohistochemistry of lesioned and grafted animals.

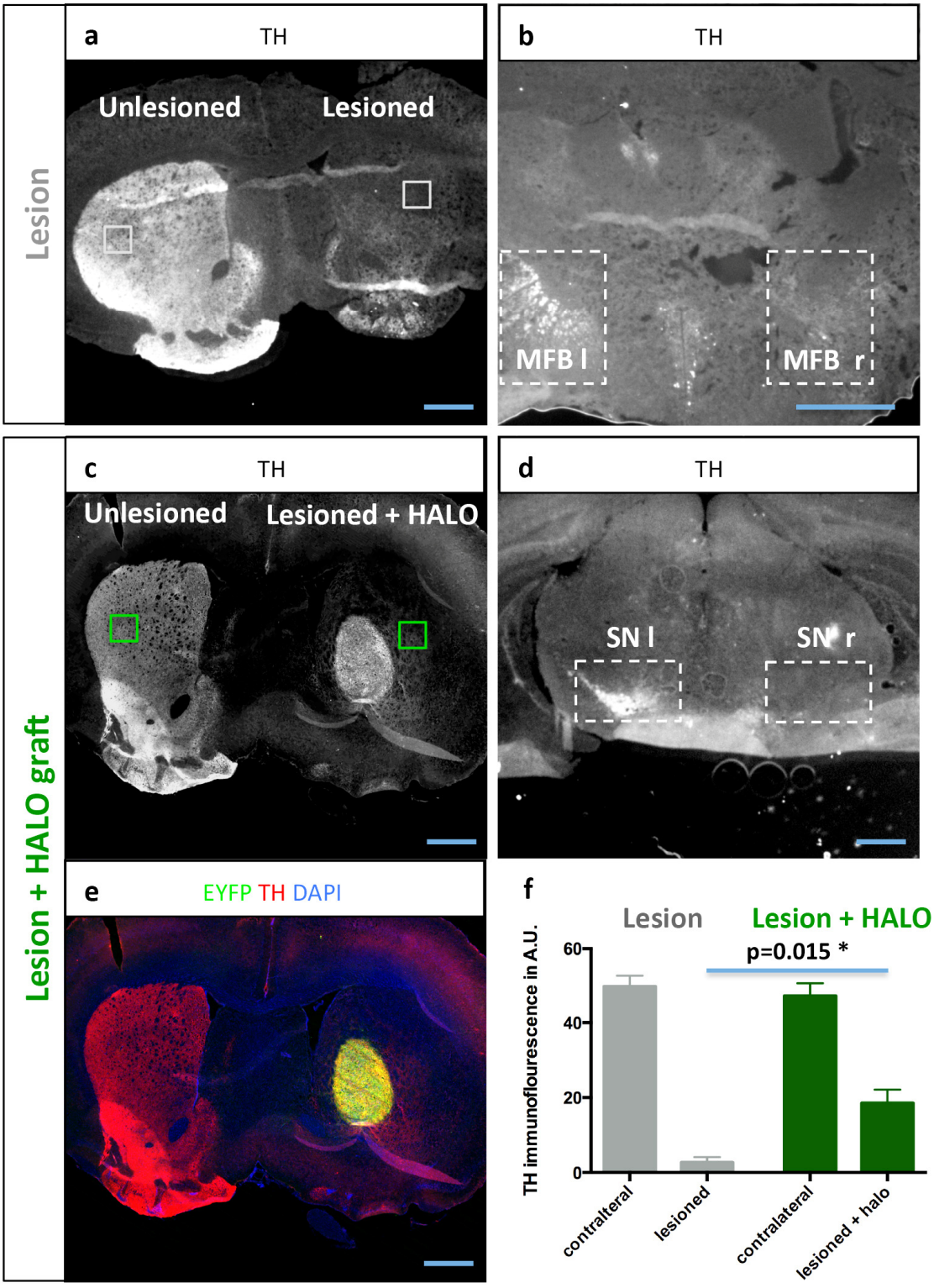

(**a, b**) Representative low power images for tyrosine hydroxylase (TH) immunofluorescence in the striatum (**a**) and at the level of the medial forebrain bundle (MFB, **b**) in a hemiparkinsonian animal 10 weeks after unilateral 6-OHDA lesion. Note the ablation of TH immunoreactivity on the lesioned side. (**c, d**) Low power images for TH immunostaining in the striatum (**c**) and at the level of the substantia nigra (SN, **d**) 6 months after grafting in a representative HALO animal. Stereological analysis of this and one other representative HALO animal showed that mesDA-rich grafts contained 8775 and 6750 TH+ neurons. (**e**) Shows EYFP (green), TH (red) and DAPI (blue) channels of the graft corresponding to (**c**). Scale bar in (**a-e**) 1000 μm. (**f**) TH immunoreactivity was quantified in the lesioned striatum and 500 μm outside the graft core in the HALO animal in areas corresponding to grey / green boxes in (**a, c**). TH immunoreactivity was partially restored in the HALO animal as compared to the lesioned animal (5.2 % in lesioned striatum vs. 39.2% in HALO-grafted striatum vs. 100% in contralateral striatum, t-test, $t = 4.08$, $p = 0.015$, error bars represent s.e.m.). A background reading from the corpus callosum was subtracted form all measurements.

Supplementary Fig. 6: Immunohistochemistry of HALO and EYFP grafts.

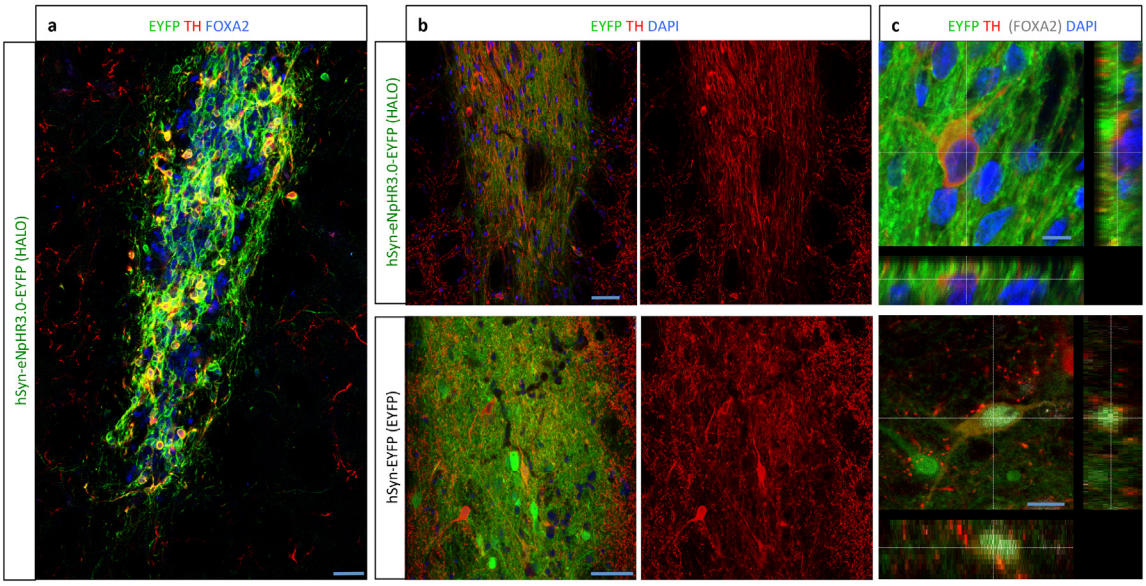

(**a**) Shows the border zone of a HALO graft at 4 weeks after transplantation. TH (red) expression is seen in a majority of HALO expressing neurons, which are embedded in a graft core of FOXA2 (blue) expressing cells. (**b**) Shows border zones of typical EYFP+/TH+ grafts 20 weeks after transplantation into 6-OHDA lesioned animals. (**c**) Shows magnified 3D confocal EYFP+/TH+ donor neurons. The cell in the lower panel co-expresses FOXA2 (grey). Nuclear counterstain is DAPI (blue) in (**b, c**). Scale bar 50 µm in (**a, b**), 10 µm in (**c**).

Supplementary Fig. 7: Electrophysiological properties of grafted human and endogenous mouse mesDA neurons.

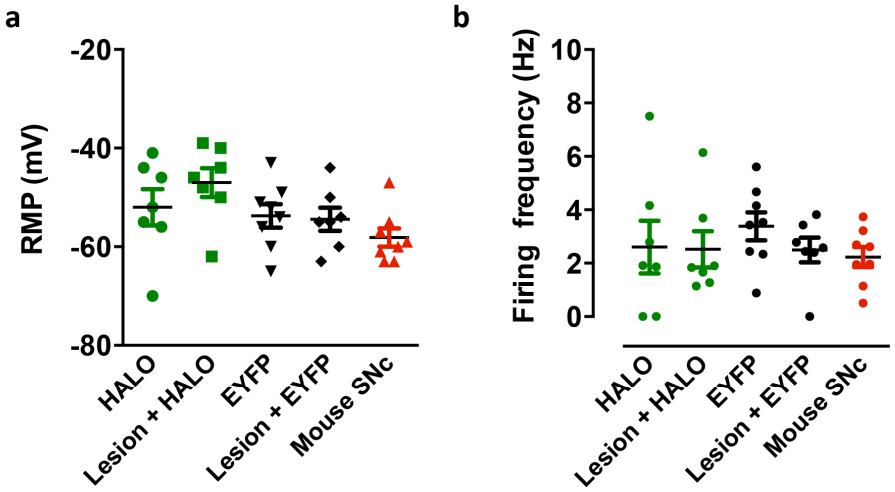

Comparison of (**a**) resting membrane potentials (RMP) and (**b**) spontaneous firing frequency (FF) recorded from human HALO- and control opsin (EYFP) expressing neurons from lesioned and unlesioned animals as well as from endogenous mouse substantia nigra pars compacta (SNc) neurons. None of the groups were statistically different from each other in one-way ANOVA (for RMP $F = 2.32$, $p = 0.08$; for FF $F = 0.51$, $p = 0.72$) and Sidak's multiple comparisons test. Given the presence of outliers we cannot rule out that some of the human neurons recorded do not exhibit mesDA neuron identity.

Supplementary Fig. 8: Immunohistochemistry of graft-derived fiber outgrowth.

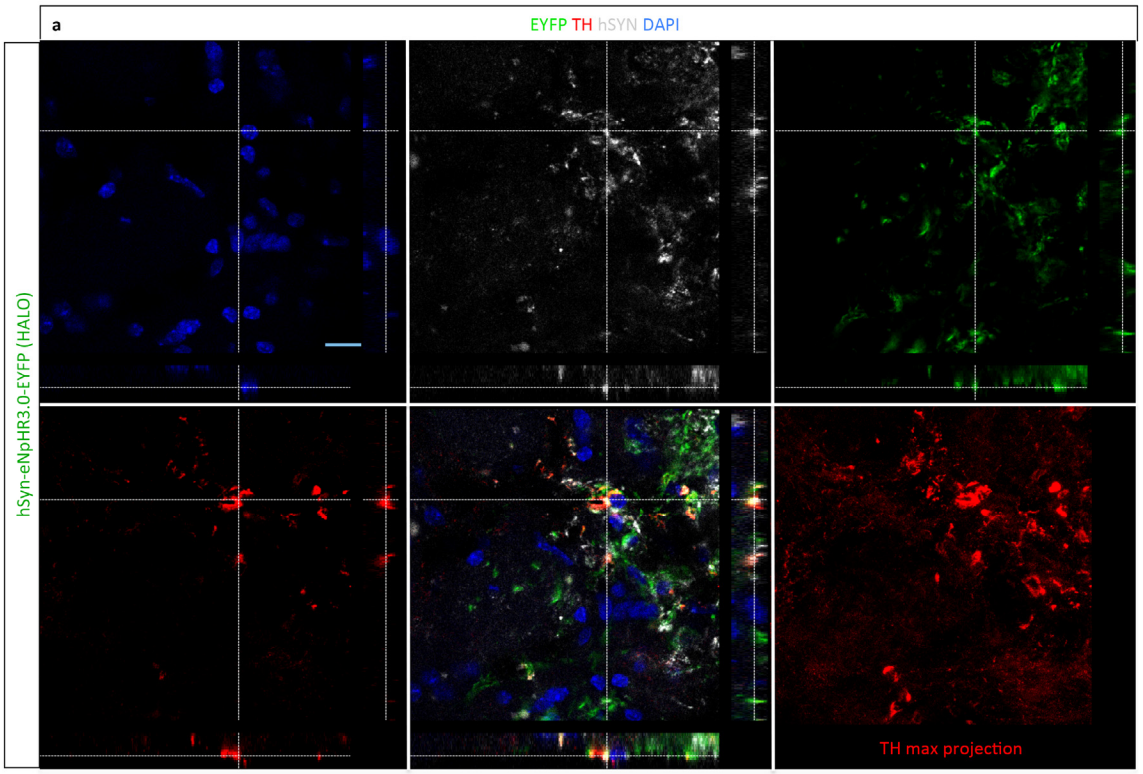

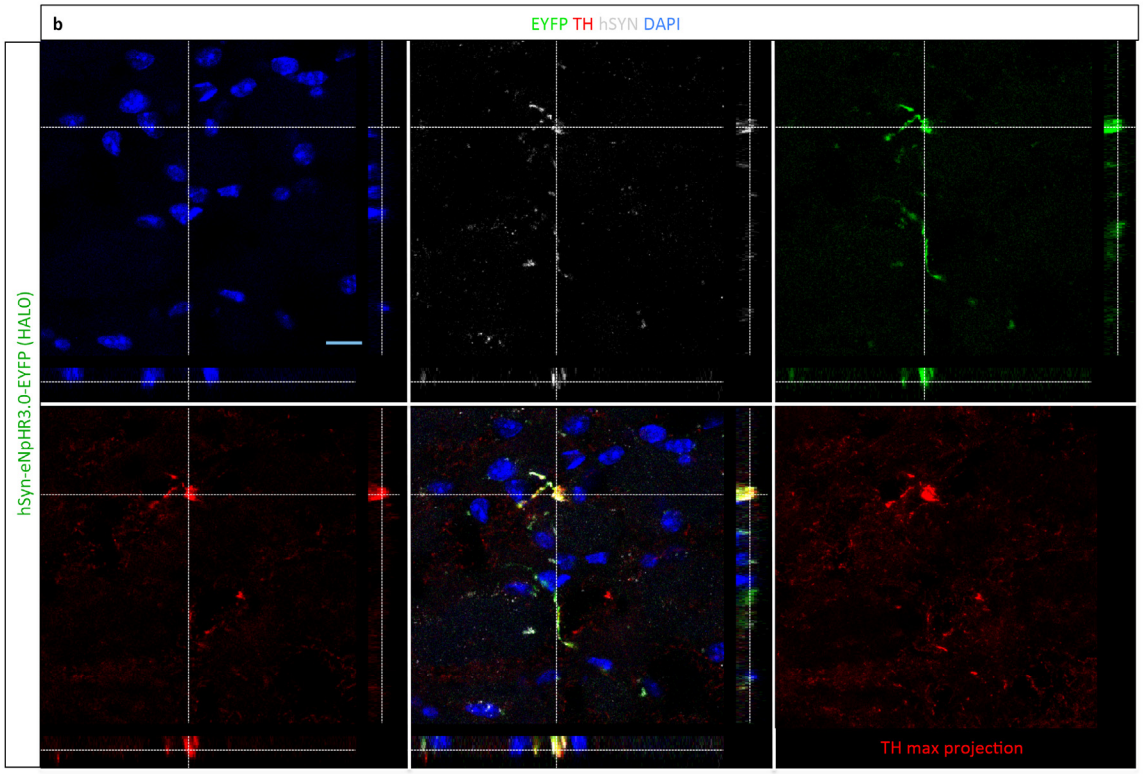

Confocal images show co-localization of TH immunoreactivity (red) with EYFP+ axons (green) and human synaptophysin (hSYN, grey) near the graft (**a**, 100 μm from the graft core) and in the dorsolateral striatum (**b**, 500 μm from the graft core) in a HALO animal. The image in the lower right represents a maximum projection of 12 confocal planes, 1 μm apart from each other for the TH staining. Nuclear counterstain is DAPI (blue). Scale bar 20 μm.

Supplementary Fig. 9: Immunohistochemistry of graft-to-host connectivity.

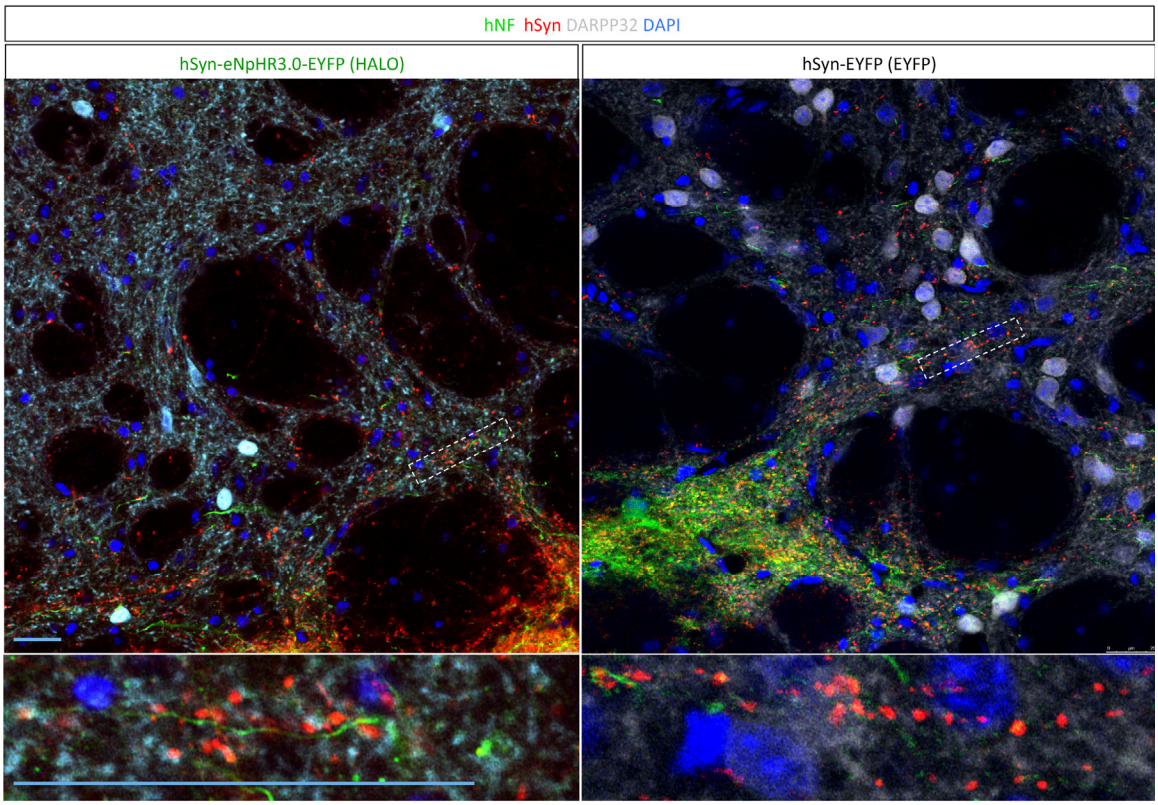

Confocal images show axons staining for human neurofilament (hNF, green) and human synaptophysin (hSYN, red) extending from grafts into the striatum. In both HALO- (left) and EYFP-animals (right) the DARPP32+ neuropil (grey) is scattered with human synaptic terminals. Maximum resolution magnifications (lower panel) show that human synaptic terminals are in direct contact with host DARPP32+ dendrites or spines. Nuclear counterstain is DAPI (blue). Scale bar 50 µm.

Supplementary Fig. 10: Whole cell current clamp recordings from MSNs in acute striatal slices.

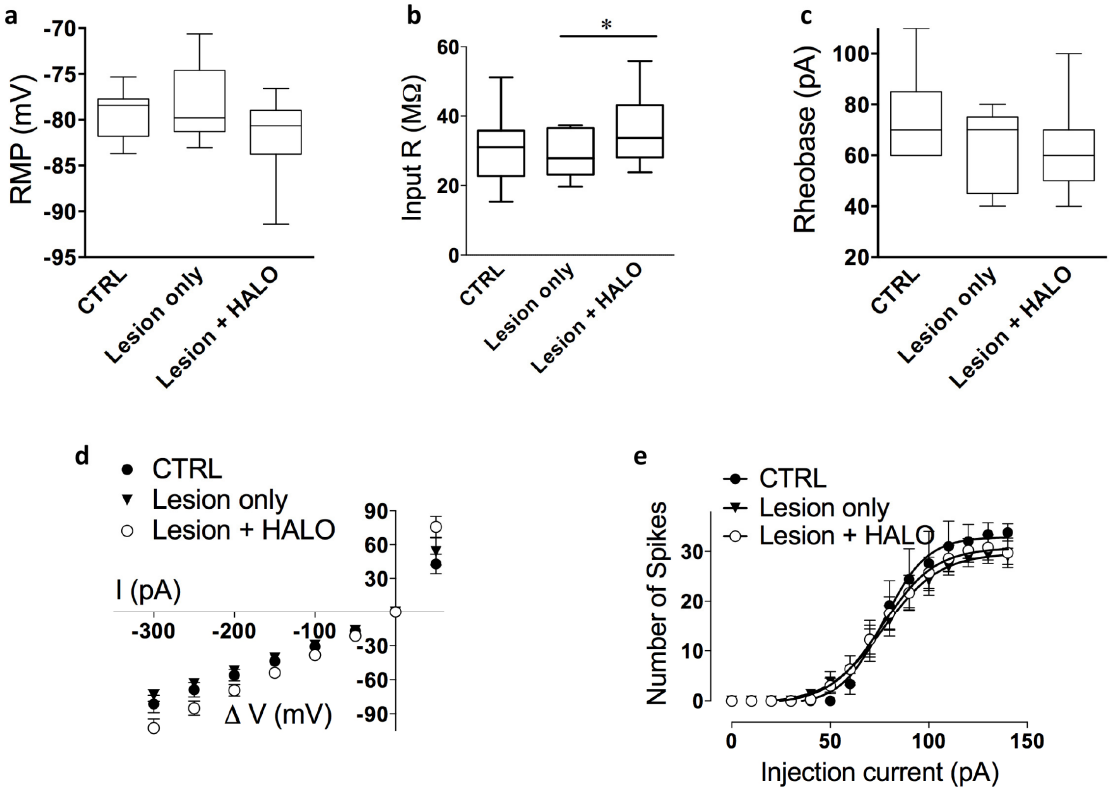

CTRL (unlesioned and non-grafted), Lesion-only and Lesion + HALO groups were compared. (**a**) Resting membrane potential, (**c**) rheobase, (**d**) current-voltage relationship and (**e**) number of spikes after current injection were not significantly different between the groups. (**b**) Only input resistance was lower in the Lesion-only group (29.2 ± 1.8 MΩ, n = 13) as compared to Lesion + HALO group (36.0 ± 2.3 MΩ, n = 18, t = 2.18, $p < 0.05$, error bars represent s.e.m.).

Supplementary Fig. 11: Cyclic voltammetry confirms dopamine release in the striatum by corpus callosum electrical stimulation.

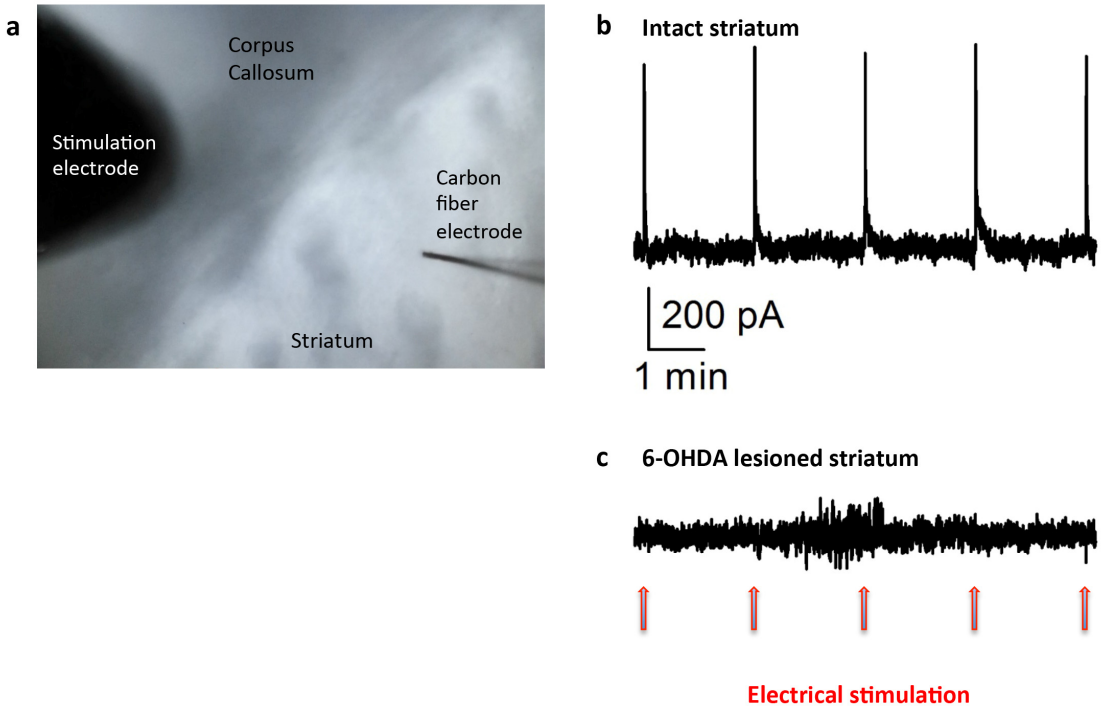

(**a**) Experimental design with the stimulation electrode placed onto the corpus callosum. The cyclic voltammetry cabon fiber electrode was placed inside the dorsal striatum where MSNs were recorded. (**b**) Shows dopamine release in the intact striatum upon each electrical stimulation (red arrow). (**c**) Shows absence of dopamine release in the 6-OHDA lesioned striatum.

Supplementary Fig. 12: Pharmacologic modulation of glutamatergic transmission onto MSNs by D1 receptor antagonism.

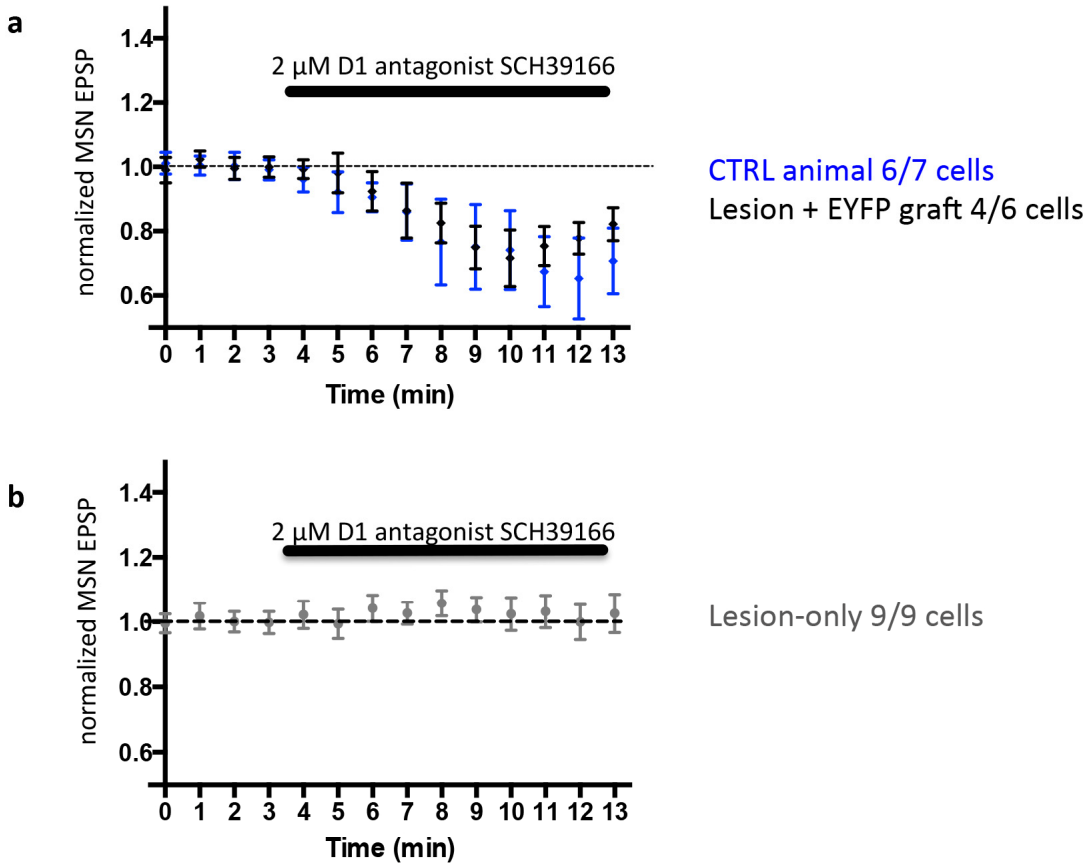

(**a**) Normalized EPSP amplitudes in medium spiny neurons (MSNs) evoked by electrical stimulation in the corpus callosum were modulated in 6/7 MSNs from CTRL animals and in 4/6 MSNs from EYFP animals by application of the D1 receptor antagonist SCH39166. (**b**) In the absence of extracellular dopamine in 6-OHDA lesioned striata D1 receptor blockade did not result in a decrease in the EPSP amplitude in 9/9 MSNs. Error bars represent s.e.m..

Supplementary Table 1: Primer pairs for analysis of transgene integration into genomic DNA.

Primer	Sequence
EYFP FW	acgtaaacggccacaagttc
EYFP RV	aagtcgtgctgcttcatgtg
eNpHR3.0-EYFP FW	atatcctgctggtggagtgg
eNpHR3.0-EYFP RV	gccacgatatccaggaaaga

Supplementary Table 2: Antibodies

Antibody	Species	Dilution	Source
GFP	Ck	1:1000	Abcam, ab13970
Tyrosine Hydroxylase (TH)	Rb	1:500	Pel-Freez, P40101-150
β-tubulin III	Rb	1:1000	Covance, PRB-435P
MAP2	Ms	1:1000	Sigma, M1406
NEUN	Ms	1:100	Chemicon, MAB377
Human Neurofilament Ho14	Rt	1:50	Trojanowski et al.
Human Synaptophysin	Ms	1:1000	Chemicon, MAB332
POU5F1/OCT4	Ms	1:200	Santa Cruz, SC5279
DARPP32	Rb	1:200	Abcam, ab40801
FOXA2	Gt	1:100	Santa Cruz, SC6554
LMX1A	Rb	1:2000	Millipore, AB10533
NR4A2 / NURR1	Ms	1:1000	R&D, PP-N1404-00

Supplementary Table 3: Raw data from the corridor test.

ID	Group	LESIONED	RECOVERED	+543nm	543 + APO
		retr l/r **frac**	retr l/r **frac**	retr l/r **frac**	
992	CTRL	-	t1 4/8 **.33**	t1 5/8 **.38**	
		-	t2 4/7 **.36**	t2 4/10 **.28**	
977	CTRL	-	t1 5/7 **.41**	t1 6/7 **.46**	
		-	t2 12/6 **.66**	t2 3/8 **.27**	
993	CTRL	-	t1 3/3 **.50**	t1 5/4 **.55**	
		-	t2 7/5 **.58**	t2 5/2 **.71**	
382	EYFP	rot. only	t1 4/7 **.36**	t1 6/5 **.54**	
		rot. only	t2 4/6 **.40**	t2 7/6 **.57**	
378	EYFP	rot. only	t1 4/7 **.36**	t1 4/7 **.30**	
		rot. only	t2 5/6 **.45**	t2 4/6 **.25**	
766	EYFP	t1 3/8 **.27**	t1 6/7 **.46**	t1 6/10 **.37**	4/2 **0.66**
		t2 2/6 **.25**	t2 7/7 **.50**	t2 4/9 **.30**	6/4 **0.6**
787	EYFP	t1 1/8 **.11**	t1 5/6 **.45**	t1 3/5 **.37**	3/5 **0.37**
		t2 2/8 **.20**	t2 4/5 **.44**	t2 4/6 **.40**	4/4 **0.5**
793	EYFP	t1 1/5 **.16**	t1 5/6 **.45**	t1 5/5 **.30**	8/5 **0.61**
		t2 2/9 **.18**	t2 8/5 **.61**	t2 5/3 **.62**	3/3 **0.5**
393	HALO	rot. only	t1 4/4 **.50**	t1 0/5 **0**	
		rot. only	t2 5/6 **.45**	t2 1/8 **.11**	
395	HALO	rot. only	t1 10/13 **.43**	t1 0/14 **0**	
		rot. only	t2 8/9 **.47**	t2 lost cannul.	
396	HALO	rot. only	t1 2/4 **.33**	t1 1/6 **.14**	
		rot. only	t2 4/7 **.36**	t2 1/8 **.11**	
915	HALO	t1 2/6 **.25** APO 4/0 **1.0**	t1 6/7 **.47**	t1 0/13 **0**	
		t2 1/10 **.09** APO 6/1 **.85**	t2 5/15 **.25**	t2 1/14 **.06**	
916	HALO	t1 2/12 **.14** APO 5/1 **.83**	t1 1/0 **excl**	t1 0/0 **excl**	
		t2 1/11 **.08** APO 6/1 **.85**	t2 7/6 **.53**	t2 0/11 **0**	
920	HALO	t1 2/9 **.18** APO 7/4 **.63**	t1 7/7 **.50**	t1 0/4 **0**	
		t2 1/11 **.08** APO 6/1 **.85**	t2 6/8 **.42**	t2 6/13 **.31**	
924	HALO	t1 2/7 **.22** APO 4/2 **.66**	t1 3/4 **.42**	t1 0/6 **0**	3/2 **0.60**
		t2 1/8 **.11** APO 6/4 **.60**	t2 4/7 **.36**	t2 1/5 **.16**	4/5 **0.44**
925	HALO	t1 2/7 **.22** APO 9/4 **.69**	t1 4/2 **.66**	t1 3/6 **.33**	4/5 **0.44**
		t2 3/9 **.25** APO 8/1 **.85**	t2 7/6 **.53**	t2 1/5 **.16**	3/3 **0.5**
943	HALO	t1 1/7 **.12** APO 5/0 **1.0**	t1 7/7 **.50**	t1 2/8 **.20**	4/4 **0.5**
		t2 2/9 **.18** APO 10/3 **.76**	t2 5/4 **.55**	t2 0/11 **0**	4/4 **0.5**

The corridor test was performed as described previously [20,21] with minor adjustments. Food restriction was limited to 95% of initial body weight and nose pokes without pellet retrieval were not counted. Sugar pellet retrievals are shown for every animal from the left (contralateral) / right (ipsilateral) side (retr l/r) and as fraction of contralateral

retrievals (frac) for both trials (t1 and t2). CTRL animals were not lesioned and not grafted. The data shown for these animals is without illumination in the recovered column and with illumination in the +543nm column. For a subset of animals pre-transplantation data from the corridor test are not available. Successful lesioning was confirmed in these animals using amphetamine-induced rotations (rot. only). Behavioral sessions with less than 4 pellet retrievals were excluded from analysis (excl). One animal lost its cannula during the second round of behavioral analysis (lost cannula). Videos from 8 complete corridor sessions were re-analyzed by two blinded raters. Despite the raters being untrained at assessing this test and the difficulties of scoring pellet retrievals on video in a relatively dark corridor, their results showed significant correlations (r^2) of 0.73 ($p < 0.01$) and 0.86 ($p < 0.001$) respectively with the live scoring results shown in this table and in main Figure 3d.

VIDEO LEGENDS:

Supplementary Video 1: Ratiometric calcium imaging of a HALO expressing D90 culture during glutamate stimulation (100 μM, 15 s pulse). 5 s/frame.

Supplementary Video 2: Ratiometric calcium imaging of a HALO expressing D90 culture during continuous glutamate stimulation (50 μM). Three inactivating 550 nm light pulses are applied, which produced a decrease in calcium levels. 1 s/frame.

Supplementary Video 3: Ratiometric calcium imaging of an EYFP expressing D90 culture during glutamate stimulation (100 μM, 15 s pulse). 5 s/frame.

Supplementary Video 4: Ratiometric calcium imaging of an EYFP expressing D90 culture during continuous glutamate stimulation (50 μM). Four 550 nm light pulses were applied without producing any change in the calcium response. 1 s/frame.

Supplementary Video 5: Corridor test. Representative recording of a CTRL animal (unlesioned and non-grafted) during optogenetic illumination showing unbiased exploration and food retrieval from both sides of the corridor.

Supplementary Video 6: Corridor test. Representative section of a Lesion-only animal showing lateralized exploration and food retrieval ipsilateral to the lesion (right side).

Supplementary Video 7: Corridor test. Representative recording of a Lesion-only animal (same animal as in video S5) injected with apomorphine showing lateralized exploration and food retrieval contralateral to the lesion (left side).

Supplementary Video 8: Corridor test. Representative recording of a recovered EYFP animal (lesioned + EYFP graft) during optogenetic illumination showing unbiased exploration and food retrieval from both sides of the corridor.

Supplementary Video 9: Corridor test. Representative recording of a recovered HALO animal (lesioned + HALO graft) during optogenetic graft silencing, showing reversion to lateralized behavior (exploration and food retrieval from right side of the corridor).

Supplementary Video 10: Corridor test. Representative recording of a recovered HALO animal (same animal as in video S9, lesioned + HALO graft + APO) during optogenetic graft silencing injected with apomorphine, showing no reversion to lateralized behavior and no contralateral overshoot.